DELAMINATION DETECTION IN THICK COMPOSITE LAMINATES USING GUIDED ULTRASONIC WAVES

A. E. Antoniou, T. T. Assimakopoulou, T. P. Philippidis*

University of Patras, Department of Mechanical Engineering and Aeronautics
P.O. Box 1401 Panepistimioupolis 265 04 Rio, Greece

ABSTRACT

An experimental investigation, using guided ultrasonic waves, was performed to detect defects in thick composite structures. The work focused on the identification of flaws encountered in wind turbine rotor blades, in-situ or during manufacturing. Delaminations between adjacent layers and shear-web debondings from blade skin were examined. Two plates with structural defects were used in the investigation. One contained an artificial delamination and the other a shear web debonding. Various excitation sources were applied e.g. broadband signals, lead breaks, Dirac pulses and discrete tone bursts produced with a wave generator. Further investigation was conducted on a delaminated wind turbine blade. The existence of the delaminations was indicated both in time and frequency domain. Fundamental flexural mode (A_0) was used to highlight the plate delamination and experimental results were compared with a plane strain FEM model. The numerical analysis corroborated the test results and enhanced the understanding of plate wave mechanics.

1. INTRODUCTION

Delamination of adjacent plies and debondings between skin and shear-webs are critical defects frequently encountered in composite structures like wind turbine rotor blades. The existence of a non-destructive method that could assess structural integrity during manufacturing or that could be used for in-situ health monitoring and detection of flaw development is of vital importance. Guided plate waves have proved a powerful tool, with the potential of scanning wider areas than conventional Ultrasonic methods. Several researchers have investigated the interaction of guided waves with delaminations in thin, up to 5 mm, CFRP composite plates. Fundamental symmetric (S_0) mode waves have been used, [1]-[3], excited by tone bursts with central frequencies of approximately 0.5 MHz, as well as flexural (A_0) mode waves [4] in the low frequency range of 20-25 kHz. Various FEM analyses, [3]-[4], have confirmed the experimental results and the delamination size and location characteristics have been investigated through parametric studies [3]. Although a lot of discussion has been made on the interaction between guided waves and delaminations, there are no reported cases in the literature concerning other structural defects, such as shear-web debondings. Moreover, there are no investigations about propagation of guided waves in thick attenuative composite laminates that structures such as large wind turbine rotor blades are usually made of.

In the present work, delaminations and shear-web debondings from the skin were studied experimentally, using guided ultrasonic waves. Two glass-fiber reinforced polyester (GRP) composite plates were thoroughly investigated. The first plate contained a nylon sheet between two adjacent layers, thus simulating a real case of delamination. Two shear-webs were attached on the other plate, one of which was locally debonded. In both cases defects could be discerned with bear eyes. Different excitations such as lead-breaks (Hsu-Nielsen sources), wideband pulses and tone bursts were applied on the structures. Tone burst frequencies ranged from 30 to 80 kHz. Normal incidence transducers were used to detect the stress waves on the plate surface. Validity of measurements and applicability of the method were then verified by additional experiments on a wind turbine blade with the same stacking sequence and thickness as the plates tested in laboratory. The blade contained an artificial delamination similar to the one existing in the first plate. FEM analysis with plane strain elements on a delaminated plate corroborated the experimental results and enhanced the

* Corresponding author; Tel/Fax: +302610-997235, e-mail: philippidis@mech.upatras.gr

understanding of the propagating plate wave modes (A_0 and S_0). All experimental set-ups highlighted the existence of the flaw. FEM and experimental results were in good agreement.

2. WAVE PROPAGATION IN MULTI-LAYERED COMPOSITE PLATES

Solving the dispersion equations derived from the generalized Navier equations (Eq. (1)) for a wave-guide medium and assuming a plane wave solution of the form (Eq. (2)), result in the plate wave modes that can propagate in the medium. Phase velocity of each mode with respect to frequency was obtained along the guidelines set in [5]. For the delaminated plate, the dispersion curves for propagation in 'P' direction, see section 3.3, are presented in Fig. 1.

$$C_{ijkl} u_{k,lj} = \rho \ddot{u}_i \ , \quad i,j,k,l = 1,...,3 \tag{1}$$

$$u_i = U_i e^{j\gamma(x_1 + \alpha x_3 - ct)} \ , \ i = 1,...,3 \tag{2}$$

C_{ijkl} is the 4^{th} order stiffness tensor, ρ the laminate effective density, u_i the displacement vector, j the imaginary unit, ω the angular frequency, c the phase velocity, γ the wavenumber ($\gamma=\omega/c$) and α the ratio of the wavenumber value for propagation in direction y over the wavenumber value for propagation in direction x, see Fig. 6. When wavelength is several times the plate thickness, the multi-layered anisotropic plate can be substituted with a homogeneously anisotropic medium with equivalent effective elastic properties [6].

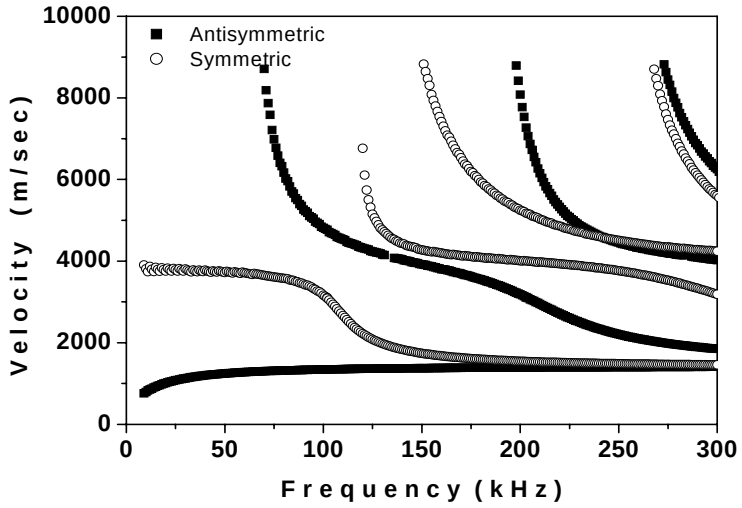

Fig. 1. Dispersion curves from the intact region of the delaminated plate

3. EXPERIMENTAL PROCEDURE

3.1 EQUIPMENT

Physical Acoustics (PAC) wave generators, C-101-HV and WAVEGEN 1410, were used to generate broadband and tone burst pulses respectively. PAC sensors R6, R15, S9208 and Panametrics V182, M2008, V413 and V133 were used either as transmitters or receivers. The pre-amplifiers used were PAC model 1220A (20-1200 kHz bandwidth). Data acquisition was performed with a PAC TRA212 DAQ-board, while sensor sensitivity was checked via PAC SPARTAN 2000 acoustic emission system.

3.2 MATERIALS

The tested plates, manufactured by hand lay-up, were made of glass-fibre reinforced polyester, 800x830 mm, with the same stacking sequence, consisting of 0^o, $\pm 45^o$ and 90^o layers, fourteen in total, at a thickness of 11 mm. In the first plate, a nylon sheet measuring 225x150 mm was placed between fifth and sixth layer, thus simulating a delamination. The shear webs of the second plate were of sandwich construction. During the experiments both plates were simply supported.

3.3 PLATE WITH DELAMINATION

Measurements took place in two directions, 'P' and 'T', as shown in Fig. 2. Distance between excitation source and the receiving sensor was kept constant, equal to 212 mm in the 'P' direction and 330 mm in the 'T' direction. Tests were conducted both in virgin and defected areas. A variety of sensor setups was utilized to define the optimal configuration. Eight measurements were conducted on undefected area and five on the area containing the delamination, both 'P' and 'T' direction. The waveforms accumulated from the tests were studied and compared to one another.

Transducer sensitivity and coupling with the plate was monitored with several 0.5 HB lead breaks, using the AE features extraction software installed in a SPARTAN 2000 AE system.

3.4 PLATE WITH SHEAR-WEBS

Tests with broadband pulse and lead break excitation, took place on the free plate surface. Shear-webs were bonded on the opposite side. The shear-web placed along line SW1 was properly bonded on the plate. The one attached under line SW2 was locally debonded (Fig. 3). Measurements were conducted in the direction parallel to the shear-webs. The transducer serving as pulser was mounted on point SW1_A, for experiments on line SW1, and on point SW2_A, for experiments along line SW2, as shown in Fig. 3. Receiver was moved away from the source in steps, placed along the corresponding shear-web axis. In the present work, measurements on two points are presented: SW1_B and SW1_C on line SW1 and SW2_B and SW2_C on line SW2. Distance between SW*_A, SW*_B and SW*_A, SW*_C points was 50 mm and 450 mm respectively.

When lead break excitation was used, receiver was permanently mounted on SW1_A for experiments along line SW1 and on SW2_A for experiments along line SW2. Lead tips were broken on the corresponding lines, moving away from the receiver in steps (SW*_B, SW*_C).

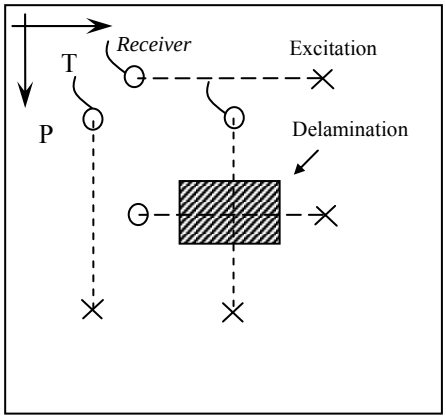

Fig. 2. Plate with delamination

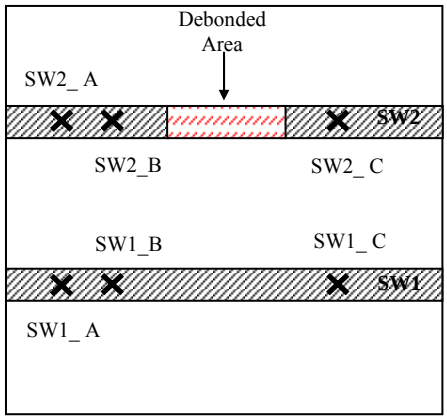

Fig. 3. Plate with two shear-webs

3.5 WIND TURBINE ROTOR BLADE

Broadband pulses were used as excitation sources. Measurements took place along the blade longitudinal axis, corresponding to the 'P' material direction of the plate structure. Delamination was 50 mm longer than the one in the plate. Distance between pulser and the receiver was kept constant and equal to 275 mm, as shown in Fig. 4. A PAC resonant sensor at 150 kHz (R15) was used as transmitter and a PAC resonant sensor at 60 kHz (R6) as receiver.

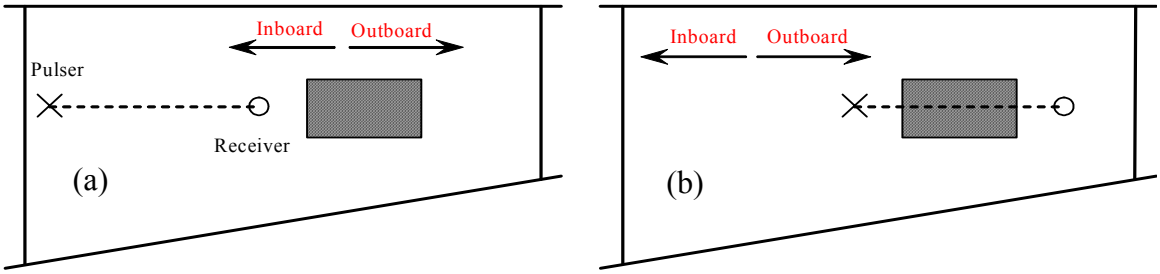

Fig. 4. Test on Wind Turbine Rotor Blade. (a) Pulser and receiver mounted outside the defected area, (b) Wavepath including the defected area

3.6 TONE BURSTS AND FEM MODEL ON THE PLATE WITH DELAMINATION

For further understanding of the wave propagation mechanics in composite plates, experiments with narrow-band excitation pulses were conducted on the delaminated plate. Four-cycle tone bursts, Fig. 5, ranging from 30 to 80 kHz were used to generate the stress waves propagating along the plate 'P' direction. Sensor placement was the same as described in section 3.3. A pair of V133 Panametrics broadband transducers served as transmitter and receiver. A plain strain FEM model was also implemented, Fig. 6, and the computed results were compared with the experimental waveforms.

ANSYS FEM commercial code was used, solving transient dynamic problems with the Newmark direct integration method. Plate material was supposed to be homogenously anisotropic with equivalent elastic properties (long wave approach) [6]. Direction 'x' (Fig. 6.) coincided with the fiber direction of 0^o layers, i.e. 'P' direction.

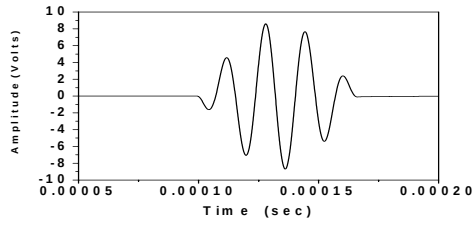

Fig. 5. WAVEGEN output. Four-cycle 60kHz tone burst

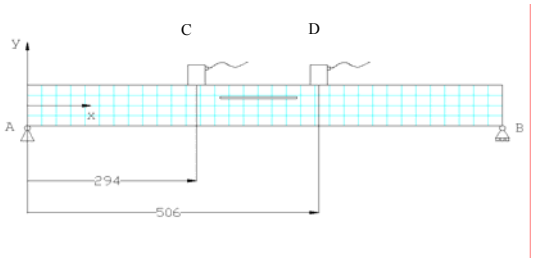

Fig. 6. FEM model of the delaminated plate

For numerical convergence, element side length was twenty times smaller than the smallest wavelength that was expected to propagate [7], [8]. Moreover, the time integration step of the Newmark method should be at least twenty times smaller than the smallest propagating time period. The selected grid consisted of 20 4-node elements (PLANE13) in the through-the-thickness direction and 1600 elements along the plate length. The structure had therefore

204186 degrees of freedom. The selected Newmark integration parameters were $\alpha = 0.2525$, $\delta = 0.5050$ and the time integration step was selected to be $\Delta t = 0.25$ μsec. The plate was 'simply supported'. The application of the 'excitation' and the calculation of vertical displacement on the plate surfaces, took place on points C and D respectively, simulating the experimental procedure.

4. RESULTS AND DISCUSSION

4.1 PLATE WITH DELAMINATION

Several sensor combinations were examined to determine the couple (pulser-receiver) that could best reveal differences between measurements on defected and undefected material. The evaluation of the transducer combinations was accomplished with the comparison and study of the acquired waveforms [9]. All measurements were plotted in graphs. Separate graphs were created for 'T' and 'P' directions of each configuration, Fig. 7. After the survey, the 'optimum' experimental set-up was established, consisting of two 60 kHz resonant PAC transducers, for both test directions. In the present work only these 'optimum' results are presented.

Reproducible signals were obtained both in the defected and undefected areas. Representative waveforms are shown in Fig 7. The delamination was clearly detected, as the waveforms changed their shape in the defected area. Especially in 'T' direction, signal amplitude decreased and the waveforms appeared to have shorter duration, when collected from the defected material. In 'P' direction, differences e.g. between maximum amplitude values or waveform duration were not obvious.

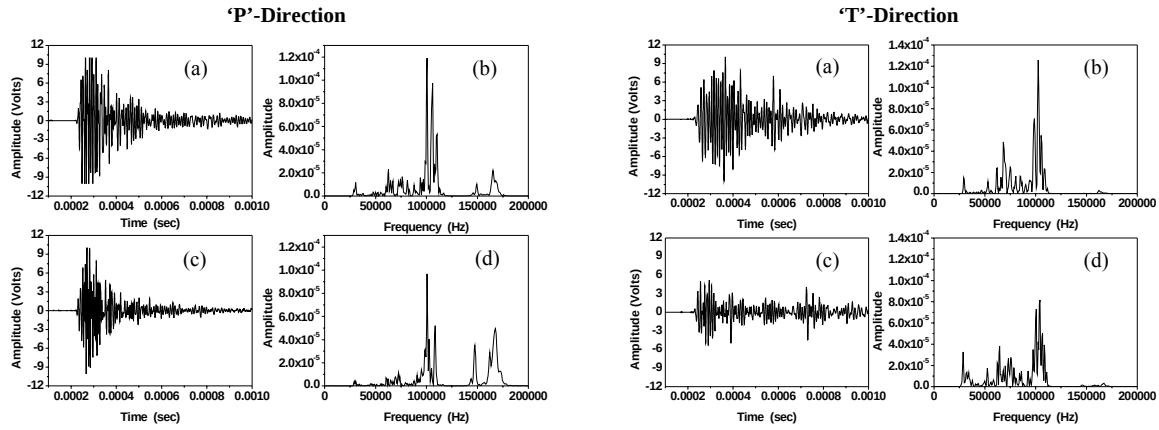

Fig. 7. Typical experiments from the delaminated plate.
Intact region (a) Representative Time series, (b) PSD transform
Defected region (c) Representative Time series, (d) PSD transform

To highlight the existence of the delamination, a Power Spectral Density transform (PSD) was applied on the signals. In 'P' direction, higher energy content at high frequencies was observed in the defected areas, while energy was reduced in the frequency range between 50 and 120 kHz. On the contrary, in 'T' direction, this could not be observed consistently. Nevertheless, an energy peak appeared near 25 kHz.

A similar study was performed with pencil lead break excitation. Reproducible signals were obtained in the defected and undefected areas, Fig. 8. Again, the resonant at 60 kHz, R6 PAC transducer was able to detect the delamination. The low frequency part of the waveform, which was also of the highest amplitude, shifted towards later arrival time, when the

wavepath included the delamination. Especially in the 'T' direction measurements, the waveform maximum amplitude decreased when tests were conducted in the defected area.

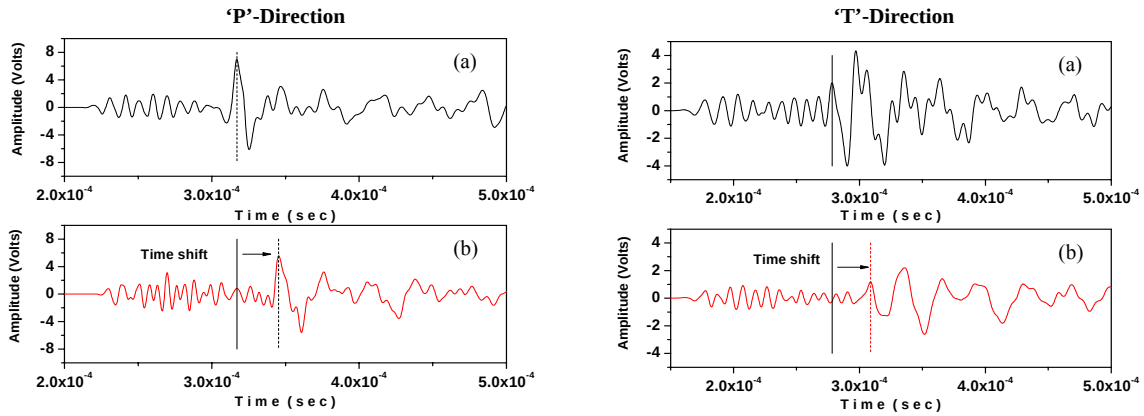

Fig. 8. Representative time series from the delaminated plate. Hsu-Nielsen excitation.
(a) Intact region, (b) Defected region

4.2 PLATE WITH SHEAR-WEBS

To detect the debonded shear-web, the previously selected couple of two resonant R6 PAC sensors was used. For the same distances between source and receiving point, waveforms acquired on properly bonded regions above the two shear-webs demonstrated obvious similarities, as presented in Fig. 9 (a,b).

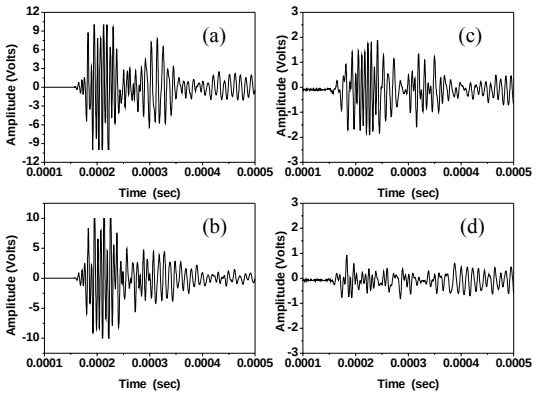

Fig. 9. Plate with shear-webs. Tests with two PAC R6 sensors serving as pulser and receiver.
(a) SW2. Pulser on SW2_A, receiver on SW2_B
(b) SW1. Pulser on SW1_A, receiver on SW1_B
(c) SW2. Pulser on SW2_A, receiver on SW2_C
(d) SW1. Pulser on SW1_A, receiver on SW1_C

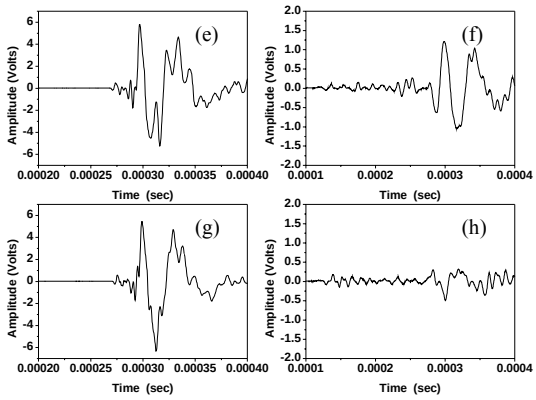

Fig. 10. Plate with shear-webs. Tests with lead breaks. PAC S9208 sensor serving as receiver.
(e) SW2. Excitation on SW2_B, receiver on SW2_A
(f) SW1. Excitation on SW1_B, receiver on SW1_A
(g) SW2. Excitation on SW2_C, receiver on SW2_A
(h) SW1. Excitation on SW1_C, receiver on SW1_A

On the contrary, waveforms changed shape in the presence of debonding (Fig. 9 (c,d)). Similar results were obtained when lead breaks were used as excitation sources. A PAC S9208 sensor was used as receiver (Fig. 10) in this case.

4.3 WIND TURBINE ROTOR BLADE

Additional experiments were performed to validate the delamination detection. Tests on a rotor blade confirmed the previous experiments on the laboratory plate. In the frequency domain, the presence of the flaw produced higher energy content at high frequencies and an energy reduction in lower frequencies, as shown in Fig. 11.

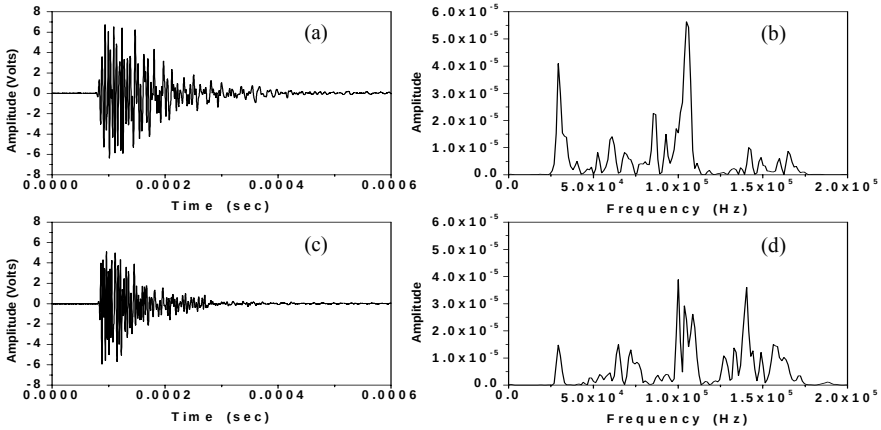

Fig. 11. Tests on a wind turbine rotor blade. Intact region (a) Time series, (b) PSD transform. Defected region (c) Time series, (d) PSD transform

4.4 TONE BURSTS AND FEM MODEL OF THE PLATE WITH DELAMINATION

The numerically calculated vertical displacements of the upper and lower surfaces of the delaminated plate revealed that at t = 100 μsec the measurement point, located in the intact area, was excited by a symmetric wave mode, as indicated by the 180^o phase difference between the two surface responses, Fig. 12a. At t = 200 μsec an antisymmetric mode was dominant, as the two surfaces at the measurement point moved in phase, Fig. 12b.

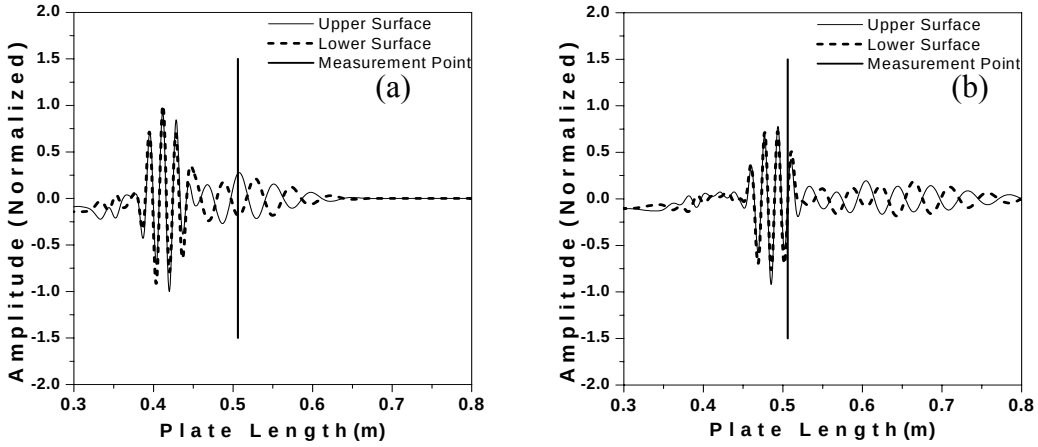

Fig. 12. Numerical results in the intact area of the 'delaminated' plate.
Intact region. (a) Wave Propagation at t = 100 μsec, (b) Wave Propagation at t = 200 μsec

The FEM model predicted the plate displacement response and was in reasonable agreement with the test results in the intact area, Fig. 13a. The symmetric and the antisymmetric modes

could be distinguished since they arrived at separate times, with the symmetric mode being faster. Moreover, the lateral mode demonstrated higher displacement values than the longitudinal mode. Test measurements on the defected area revealed a time shift of the flexural mode towards later arrival time, compared to the waveforms collected on virgin area, and also an amplitude reduction in the presence of the delamination, Fig. 13b. The delay of the lateral mode and its attenuation were numerically predicted, Fig. 13 (c,d), although there was not an exact coincidence between experimental and calculated waveforms, Fig. 13c. For comparison purposes, experimental and numerically calculated waveforms were normalised with respect to the waveform obtained in the intact area maximum amplitude.

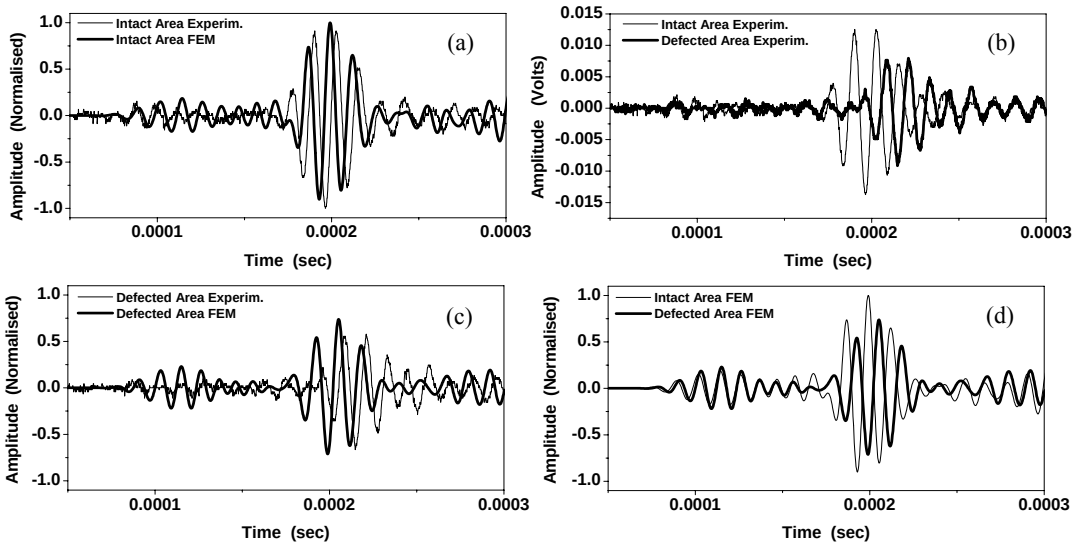

Fig. 13. Plate with delamination. FEM and experimental results with 80 kHz four-cycle tone burst excitation. (a) Experiment and FEM. Intact Area. Normalized results, (b) Experiment. Defected and Intact Area, (c) Experiment and FEM. Defected Area. Normalized results, (d) FEM. Defected and Intact Area

Experimentally measured phase velocity of the flexural mode coincided with the phase velocity calculated with the FEM model and the phase velocity of the A_0 mode numerically calculated from theory of Elasticity [5], as shown in Fig. 14.

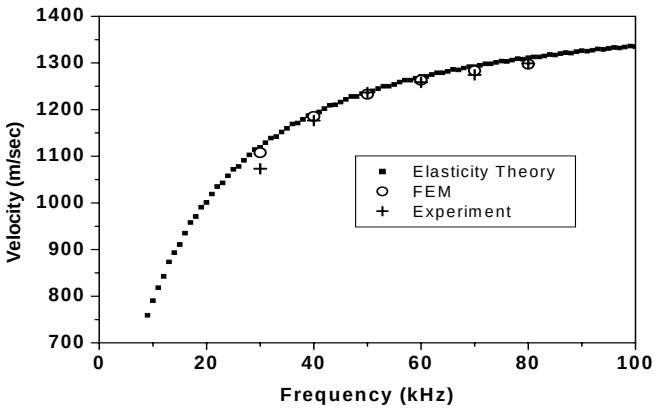

Fig. 14. Dispersion curve of the composite plate lowest antisymmetric mode (A_0)

Phase velocity was measured using two receivers, placed along the same line with the excitation source. Two waveforms were thus acquired in each measurement, one with each sensor. The time delay between corresponding peaks of the flexural mode, e.g. the third peak of each signal, was calculated. Phase velocity measured from the third peak was determined as the distance of the receivers over this time delay. An average of these phase velocity values from all the peaks of the flexural mode was considered as the A_0 phase velocity at the corresponding frequency.

The presence of the delamination reduces the laminate capability of carrying transverse shear loads. Reducing the C_{55} effective stiffness term of the plate, to 90% and 70% of the initial value of the intact structure, the variation of the phase velocity of the A_0 mode was studied, Fig. 15. Lower stiffness resulted in lower A_0 mode phase velocities, thus explaining the time shift of the lateral mode when the wave path crossed the defected area. Consequently, for the GRP plate configuration examined, the behaviour of the fundamental antisymmetric mode was directly correlated with the presence of the delamination.

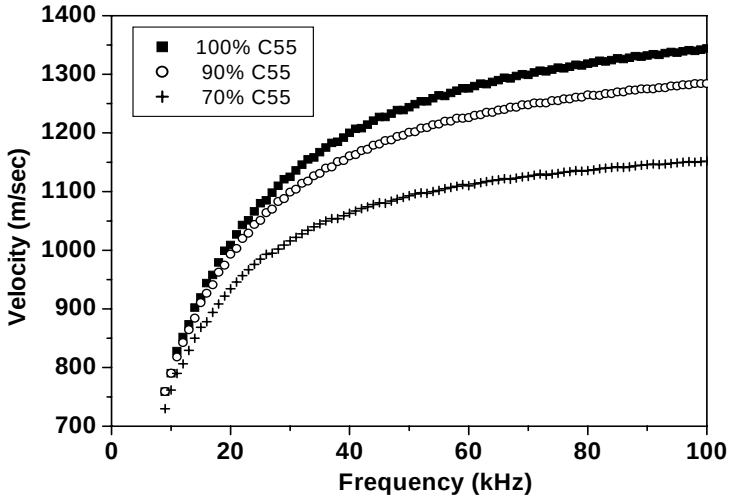

Fig. 15. Phase velocity variation of the lowest antisymmetric mode (A_0) of the examined plate, predicted with the theory of Elasticity

5. CONCLUSIONS

With guided ultrasonic wave testing, flaws were identified in thick composite plate-like structures such as wind turbine rotor blades. Experiments conducted with the R6-R6 sensor combination in the direction of the maximum material stiffness of the delaminated plate, 'P', revealed higher energy content at high frequencies and an energy reduction in the low frequencies, in the presence of delamination. No differences appeared in the maximum amplitude or duration compared to the waveforms obtained in the intact region. On the other hand, in 'T' direction, signals acquired in the delaminated area demonstrated a significant amplitude decrease. Lead break excitation showed a shift of the low frequency part of the waveform, towards later arrival time, when a flaw was present between source and receiver.

From the experiments on the plate with the shear-webs, it was observed that the time signals were more attenuated above a properly bonded shear-web than along the debonded one. This was attributed to the existence of the shear-web that added flexural stiffness and restricted lateral motion.

Measurements were also conducted on a rotor blade, in 'P' direction. The blade contained an artificial delamination and in the defected area had the same stacking sequence with the aforementioned plates. Signal was more attenuated in the presence of the delamination than in the intact area. Time series transforms to the frequency domain confirmed the results obtained

on the plate. At high frequencies, higher frequency content was observed in signals acquired inside the delaminated area than in these from the undefected region.
Two different wave modes propagated in the plate for frequencies below 80 kHz, the fundamentals A_0 and S_0. Delamination was highlighted using the propagation of the A_0 antisymmetric mode. The waveform was significantly altered when the wavepath crossed the defected area, since the transverse shear stiffness of the plate was reduced. The wave packet was shifted towards later arrival time and, above 60 kHz, it demonstrated a decrease in amplitude values compared to the time series acquired in virgin regions.

ACKNOWLEDGEMENTS

This study was partially supported by DG XVII of EC through funding of JOULE III, # JOR3-CT98-0283 'Acoustic Emission Proof Testing and Damage Assessment of Wind Turbine Blades (AEGIS)'. The authors are also indebted to Theodore Kossivas of Geoviologiki S.A. for providing laboratory test specimens and access for rotor blade measurements.

References

1. **Guo N.** and **Cawley P.,** 'Lamb wave propagation in composite laminates and its relationship with acousto-ultrasonics', NDT&E International, **26**/2 (1993), 75-84.
2. **Tan K. S., Guo N., Wong B. S.** and **Tui C. G.,** 'Experimental Evaluation of Delamination in Composite Plates By the Use Of Lamb Waves', **53** (1995), 77-84.
3. **Guo N.** and **Cawley P.,** 'The interaction of Lamb waves with delaminations in composite laminates', J. Acoustic Society of America **94**/4 (1993), 2240-6.
4. **Diamanti K., Hodgkinson J. M.** and **Soutis C.**, 'Damage Detection of Composite Laminates Using PZT Generated Lamb Waves', Proceedings of the First European Workshop on Structural Health Monitoring 2002, Ed. D. Balageas, DESTech Publications, 398-405.
5. **Nayfeh A. H., Chimenti D. E.,** 'Free Wave Propagation in Plates of General Anisotropic Media', Applied Mechanics, **56** (1989), 881-886.
6. **Sun C. T., Sijian L.,** 'Three-Dimensional Effective Elastic Constants for Thick Laminates', J. Comp. Mat., **22** (1987), 629-639.
7. **Moser F., Jacobs L. J.** and **Qu J.,** 'Modeling Elastic Wave Propagation in Wavequides With the Finite Element Method', NDT & E Int., **32** (1999), 225-234.
8. **ANSYS Theory Manual**
9. **Philippidis T. P., Antoniou A. E., Assimakopoulou T. T.**, 'AU-Evaluation of Defected GRP Structures', Project report AEGIS JOULE III #JOR3-CT98-0283 (2002).